

Cosmological Simulations of X-ray Clusters: The Quest for Higher Resolution and Essential Physics

Michael L. Norman

UC San Diego, 9500 Gilman Dr, La Jolla, CA 92093-0424

Abstract. I review cosmological simulations of X-ray clusters. Simulations have increased in resolution dramatically and the effects of radiative cooling, star formation feedback, and chemical enrichment on the ICM are being simulated. The structure and evolution of non-radiative X-ray clusters is now well characterized. Such models fail to reproduce the observed $L_x - T$ relation, implying the need for additional physics. Simulations adding radiative cooling produce too much cool gas and unreasonably high X-ray luminosities. Simulations including star formation and feedback appear more promising, but need further refinement. New observations should help in this regard.

1 Introduction

As the largest gravitationally bound objects in the universe, clusters of galaxies have attracted the attention of observers and numerical simulators alike. For over a decade, beginning with the pioneering hydrodynamic simulations of Evrard (1990), numerical simulations have been used to understand the physics of X-ray cluster formation and to predict their abundance at high redshift which is a sensitive probe of cosmology (see review Henry in these proceedings.) Observationally, clusters of galaxies have historically been studied in the optical and X-ray portions of the EM spectrum (Forman & Jones 1982). X-rays in particular provide an unambiguous method for detecting clusters at low and intermediate redshift, and many surveys have been conducted (Henry, these proceedings.)

A number of groups have simulated the formation of statistical ensembles of X-ray clusters (Kang et al. 1994; Bryan et al. 1994a,b; Bryan & Norman 1998; Eke, Navarro & Frenk 1998; Yoshikawa, Jing & Sato 2000) in order to provide a theoretical bridge between what is observed—the X-ray luminosity function (XLF) and X-ray temperature function (XTF)—and the cluster mass function (CMF). The CMF in turn is directly related to the matter fluctuation power spectrum $P(k)$ —one of the holy grails of observational cosmology. In so doing, simulators have discovered that X-ray clusters are not the simple gas-bags they were once thought to be. It has been found that quite high resolution is required to converge on the predicted properties of non-radiative clusters (Anninos & Norman 1996; Frenk et al. 1999), and that the inclusion of

radiative cooling and other non-adiabatic effects strongly affects the clusters' emission and structural properties (e.g., Pearce et al. 2000).

This review will follow the development of cosmological simulations of X-ray clusters primarily from a historical perspective, starting with the non-radiative simulations of Evrard (1990) and others and concluding with current models incorporating cooling, star formation, supernova feedback and chemical enrichment. The field has been enlivened by the arrival of new observations and new questions. I will attempt to keep the questions at the forefront of this review, for while some have been convincingly answered, many are still open. Simulations of cluster mergers done outside the framework of CDM-driven structure formation are not reviewed here for space reasons.

2 Methodology

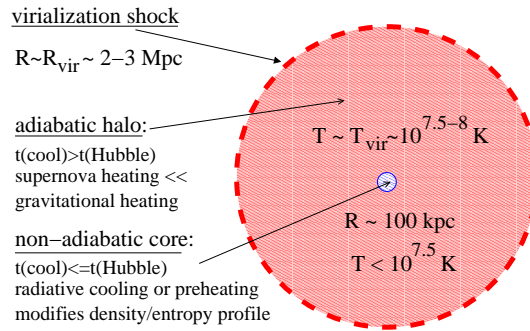


Fig. 1. Simplified structure of a bright X-ray cluster.

From a purely technical perspective, simulating X-ray clusters has been a quest for higher resolution and essential physics. This quest is still ongoing. Here I outline some of the basic requirements for simulations of this sort, describe how they are performed, and how they have advanced over the past decade.

Fig. 1 shows a simplified model of an X-ray cluster. It is a gross generalization based both on our models of hierarchical structure formation and observations of real X-ray clusters. As intergalactic gas falls into the potential well of the cluster, it passes through several strong shocks, the innermost of which is called the virialization shock. The virialization shock is located about one virial radius from the cluster center and it heats the gas to $T \sim \frac{1}{2} T_{\text{vir}}$. Typical numbers for a Coma-like cluster are $R_{\text{vir}} \sim 2-3 \text{ Mpc}$, $T_{\text{vir}} \sim 10^8 \text{ K}$. Inside the virialization shock is the hot intracluster medium we observe in X-rays. The bulk of the X-ray halo is adiabatic insofar as $t_{\text{cool}} = c_v \rho T / \Lambda_x(T) > t_{\text{Hubble}}$. Here $\Lambda_x(T)$ is the bolometric X-ray emissivity

of the gas. Inside the adiabatic halo is a non-adiabatic core where densities are high enough to reverse the inequality. In the core, radiative cooling and possibly other processes have modified the entropy of the gas. The bulk of a cluster's luminosity is emitted from the core region, which is observed to have a radius of 100 – 200 kpc (Sarazin 1986).

Numerical simulations of cluster formation follow the growth of density perturbations in the gas and dark matter subject to self-gravity and cosmic expansion. The density perturbations are initialized as a Gaussian random field with a power spectrum $P(k)$ taken from linear theory and constrained by observations (e.g., Tegmark & Zaldarriaga 2002). The simulation volume is typically cubic and periodic boundary conditions are assumed. The free parameters in these simulations are the usual cosmological ones: $h, \sigma_8, \Omega_d, \Omega_b, \Omega_\Lambda$. Evolving the density perturbations into the nonlinear regime requires solving the equations of gas dynamics and dark matter dynamics subject to their mutual self-gravity in a frame comoving with the expanding universe. Both N-body and grid methods are used for this purpose (see review by Bertschinger 1998.) These simulations must be done in 3D, making them computationally expensive.

In order to accurately predict the X-ray luminosity of a simulated cluster, the density and temperature distribution of gas within the core must be resolved (Annis & Norman 1996). Ten resolution elements (grid points or SPH smoothing lengths) in a core radius would be ideal; three would be marginal. Here is where the central difficulty arises. A Coma-like cluster forms due to infall of material within a Lagrangian volume of radius ~ 15 Mpc comoving. Thus the minimum box size would be 30 Mpc on a side. Taking 30 kpc as the minimum useful resolution, we see that any simulation will need a spatial dynamic range of 1000 but preferably three times that. However, in order to adequately sample the large-scale tidal field which affects how the cluster collapses, a box 100 Mpc on a side is needed. The required spatial dynamic range is thus 3,300 (marginal) or 10,000 (ideal). Simulations aimed at computing cluster statistics (i.e., XLF or XTF) would need even larger volumes (250-500 Mpc) and concomitantly higher spatial dynamic range.

Simulations employing uniform Eulerian grids cannot achieve such dynamic ranges because the memory requirement scales as the cube of the number of grid points. Grids of 1024^3 are at the limit of the resources of even the largest parallel supercomputers. Instead, researchers employ numerical methods with variable and/or adaptive resolution. Two principal methods have been used: smoothed particle hydrodynamics (SPH), a gridless particle-based method that tracks the Lagrangian motion of fluid particles (Evrard 1990; Thomas & Couchman 1992; Katz & White 1993; Metzler & Evrard 1994; Navarro, Frenk & White 1995; Sugimotohara & Ostriker 1998; Lewis et al. 2000; Pearce et al. 2000; Valdarnini 2002) and a number of grid-based methods employing static-nested or adaptive Eulerian mesh hierarchies (Annis & Norman 1996; Bryan & Norman 1997; Loken et al. 2002) or quasi-

Lagrangian deformable meshes (Gnedin 1995; Pen 1995). Of the mesh-based methods, adaptive mesh refinement (AMR; Bryan 1999; Bryan & Norman 1999) appears to be the most powerful. A comparison of 12 codes embracing all these methods on the formation of the “Santa-Barbara Cluster”—a Coma-like cluster in a standard CDM universe—showed that AMR and SPH produce comparable results at comparable resolution (Frenk et al. 1999).

Until rather recently, cluster simulations have assumed the gas is non-radiative because this is the simplest assumption one can make and it is approximately true. In such simulations, shock waves and turbulent mixing of fluid elements are the only mechanisms which change the entropy of the gas. Despite this simplification, convergence on the properties of so-called adiabatic clusters (a misnomer) has been difficult for reasons of resolution and the numerical treatment of shock waves (Frenk et al. 1999). The effects of turbulent mixing has scarcely been addressed (but see Norman & Bryan 1998). Next in the chain of complexity is the addition of radiative cooling into the gas energy equation. A number of authors have carried out simulations including radiative cooling with interesting albeit divergent results, as discussed below. Even more ambitious is the inclusion of a recipe for star formation and feedback (energy and metals) from galaxies. Simulations of this sort are in their infancy, but show some promise to recover the properties of real clusters (cf. Valdarnini 2002).

3 Simulations of Non-radiative Clusters

3.1 Can We Make Coma?

Evrard (1990) carried out the first hydrodynamic cosmological simulations of X-ray cluster formation in a standard CDM model. His motivations were twofold: first, to study how a rich cluster of galaxies is assembled in hierarchical models, and second, to see if the resulting cluster resembled Coma. The code employed (Evrard 1988) coupled a variable smoothing length implementation of SPH to a P³M N-body solver for the dark matter. With only 4096 particles (32^3) each for gas and dark matter fields, the spatial resolution in the cluster core was 200 kpc. While insufficient to resolve the cluster core, the simulations established a number of results that have been confirmed by subsequent, higher resolution simulations. First, that the cluster forms at the intersection of filaments of dark matter and gas by the mergers and accretion of subclusters. Second, that inside the virial radius, the gas is *approximately* isothermal and in hydrostatic equilibrium, thus justifying two key assumptions made in the isothermal β -model introduced by Cavaliere & Fusco-Femiano (1976) to fit X-ray cluster brightness profiles. A third interesting result was that residual kinetic energy in the gas and anisotropy in the dark matter velocity distribution function biases cluster mass estimates made using the β model on the low side by 30%. Subsequent studies have shown that the magnitude of this bias is sensitive to numerical resolution

and the dynamical state of the cluster (Evrard, Metzler & Navarro 1996). Finally, that the integrated cluster properties and synthetic X-ray maps were encouragingly similar to Coma and A2256, suggesting that models of this kind were on the right track.

Thomas & Couchman (1992), with their own implementation of SPH+P³M achieved an impressive 20 kpc resolution in the center of the cluster with 2×32^3 particles by drastically dropping the force softening length and SPH minimum smoothing length. This they did at the risk of introducing spurious two-body relaxation effects which they analyzed in detail. Confident that the effect was not present, they found that the gas density profile formed a flattened central core, while the DM profile possessed a central cusp. This latter finding foreshadowed the discovery of a universal dark matter density profile in CDM simulations by Navarro, Frenk & White (1997), but was not focussed on. Rather, the authors commented that “the outer profiles match very well”.

3.2 Cluster Scaling Laws

Kaiser (1986) showed that in the absence of non-gravitational heating/cooling, the ICMs of X-ray clusters of different masses and formation epochs should be self-similar. Kaiser derived scaling laws relating the mass, radius (and hence density), temperature, and DM velocity dispersion for a top-hat density perturbation collapsing and virializing at redshift z . Namely: $T(M, z) \propto M^{2/3}(1+z)$ and $L_x(M, z) \propto M^{4/3}(1+z)^{7/2}$. A direct consequence of these scaling laws is that at fixed redshift, L_x should scale as T^2 . Observations, however, are consistent with $L_x \propto T^3$ with substantial scatter (David et al. 1993). Since simulations showed that clusters form hierarchically, it is reasonable to ask whether Kaiser’s scaling laws are still obeyed.

With this motivation, Navarro, Frenk & White (1995) simulated the formation of 6 clusters of different masses drawn from a single, large box standard CDM simulation. Their procedure was innovative: the initial data for each cluster was resampled at higher resolution and then evolved within the large-scale tidal field. The simulations were performed with SPH coupled to an N-body tree code with a force softening length of 100 kpc. This study yielded several important results. First, that the density profiles for both gas and dark matter when plotted as overdensities versus radius in units of the virial radius exhibited self-similar behavior. Second, that the gas and dark matter profiles showed no evidence of a central core, but rather exhibited a logarithmic slope that steepens from ~ -1 near the center to -3 near the edge. They introduced a fitting function for the dark matter profile whose general form we now refer to as an NFW profile:

$$\rho(r)/\rho_{crit} = \frac{\delta_c}{(r/r_s)(1+r/r_s)^2}$$

where r_s is a scale radius and δ_c is a characteristic density. They studied the formation history of their six clusters and found that while merger histories

differed considerably from cluster to cluster, all clusters gained the majority of their mass between $z=1$ and $z=0.2$. Finally, they confirmed that their clusters obeyed Kaiser's scaling laws and concluded that the central properties of the intracluster medium are determined by non-gravitational processes such as radiative cooling or pre-heating at high redshift.

3.3 Numerical Resolution and the $L_x - T$ Relation

In 1994 several papers appeared (Kang et al. 1994; Bryan et al. 1994a,b) which attempted to compute large statistical samples of non-radiative X-ray clusters using Eulerian grid codes combining two higher order-accurate gas dynamics algorithms (TVD, PPM) with a particle-mesh dark matter solver (Ryu et al. 1993; Bryan et al. 1995). The advantage of these methods relative to SPH are their speed, allowing larger grids and particle counts for the same computer resource, and superior shock-capturing ability. A disadvantage relative to SPH is that the spatial resolution is limited by the grid spacing Δx , which is fixed. As discussed above, achieving even 30 kpc resolution in cluster cores is not feasible with current computers without resorting to nested or adaptive grids. Nonetheless, Bryan et al. (1994b) simulated a large sample of X-ray clusters in a cold+hot dark matter (CHDM) universe at low resolution and found that the simulated clusters obeyed $L_x \propto T^3$, in agreement with observations but at odds with Kaiser's scaling laws. Was this a result of new physics (massive neutrinos) or numerical resolution, as suggested by Navarro et al. (1995)?

Anninos & Norman (1996) carried out a resolution study of non-radiative X-ray clusters using a nested-grid Eulerian cosmological hydro code and found that while the mass-weighted cluster temperature was a weak function of resolution, the X-ray luminosity was very sensitive to resolution, scaling as $L_x \propto \Delta x^{-1.1}$ for $1 \leq \Delta x(Mpc) \leq 0.1$. This dependence is a consequence of under-estimating the central gas density due to resolution effects and thereby under-estimating the X-ray emissivity in the cluster core. Bryan & Norman (1998) used this scaling law to correct the predicted luminosities for three statistical samples in three cosmologies (SCDM, CHDM, OCDM) computed at 300 kpc resolution and found good agreement with Kaiser's (1986) scaling laws and the results of Navarro, Frenk & White (1995). The discrepancy in the predicted $L_x - T$ relation was thus explained as an artifact of poor resolution. However, although all simulations now agreed, they still disagreed with observations.

3.4 The Santa Barbara Cluster Test Project

By the late 1990s, a number of groups had developed codes capable of resolving the core structure of non-radiative clusters. The structure of non-radiative clusters is now fairly well determined. The definitive study was the Santa Barbara Cluster Comparison Project (Frenk et al. 1999) in which the results of

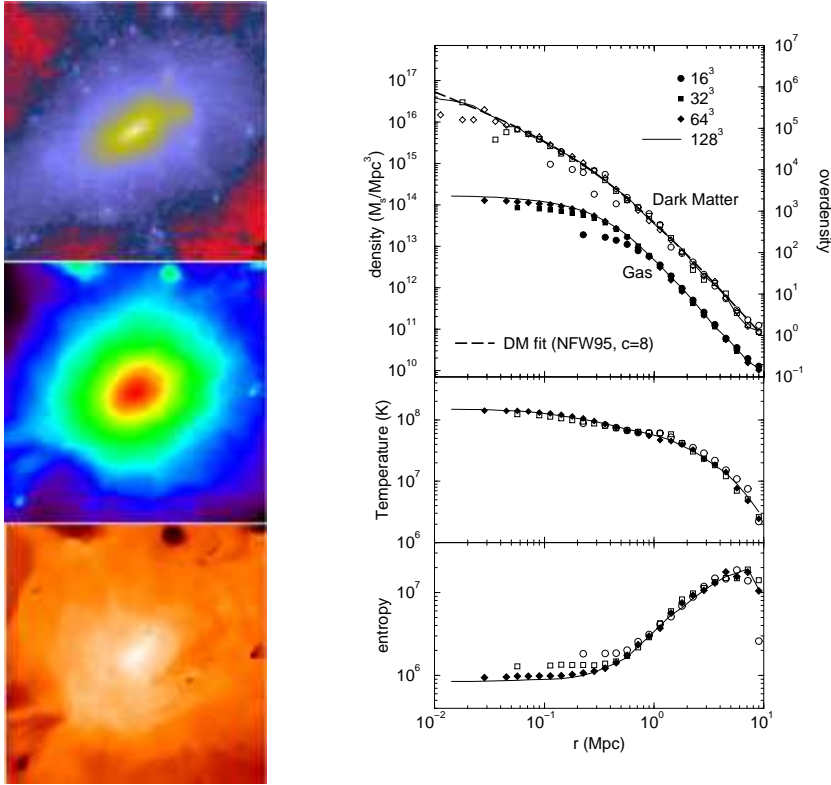


Fig. 2. AMR simulation of the Santa Barbara cluster. *Left, from top to bottom:* projections of dark matter density, gas density, and emission-weighted temperature in a 5 Mpc field centered on the cluster. *Right:* Radial profiles of spherically averaged quantities, from Bryan & Norman (1997).

12 codes implementing seven different numerical algorithms were compared for Coma-like cluster forming in a standard CDM cosmology from identical initial conditions. Among codes capable of resolving the core radius of the gas distribution, X-ray luminosities agreed to within a factor of 2. All codes regardless of resolution agreed to within 10% on the mass and average temperature of the cluster. This implies that simulations can predict the XTF to much higher precision than the XLF, ignoring the effects of other physics.

Fig. 2a shows an AMR simulation of the Santa Barbara cluster with a spatial dynamic range of 8,192 (Bryan & Norman 1997). This corresponds to a resolution of 7.8 kpc inside the cluster core within a 64 Mpc cube. Note that the dark matter halo is elongated while the gas distribution is more spherical due to the isotropizing effect of gas pressure. The virialization shock can be seen as a discontinuity near the edge of the temperature image. Fig. 2b shows spherically averaged radial profiles of various quantities from the same

simulation. These results were included in the Santa Barbara comparison and are representative of the high resolution results. The dark matter profile is well fit by an NFW profile with concentration parameter $c=8$. At high resolution, the gas density profile tracks the NFW profile at large radii but has a flat core at small radii $r < 0.1r_{vir}$. The entropy-related variable $T/\rho^{2/3}$ also exhibits a flat core, but rises linearly with radius outside the core. The temperature profile exhibits a substantial gradient at large radii and continues to rise, albeit more slowly, as $r \rightarrow 0$.

3.5 Cluster Temperature Profiles

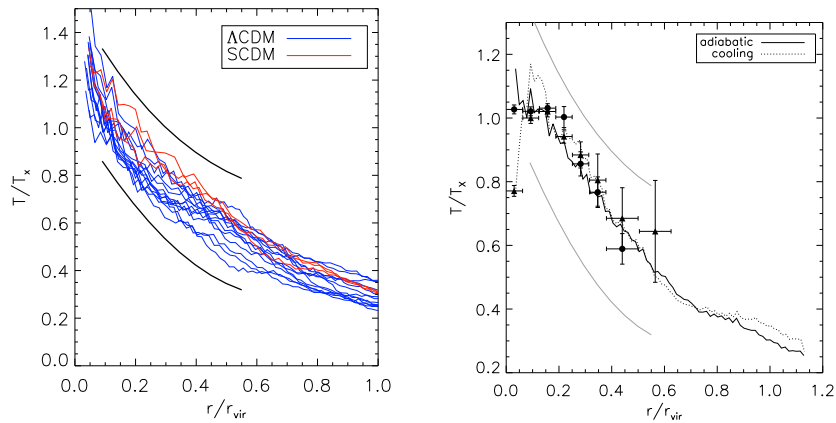


Fig. 3. (a) Universal temperature profile from AMR simulations non-radiative, relaxed clusters in two cosmologies, (b) Comparison of numerical predictions with recent *BeppoSAX* data (De Grandi & Molendi 2002). In both figures, the black solid lines are the 1σ confidence band from Markevitch et al. (1998). From Loken et al. (2002).

Early observations and numerical simulations suggested that ICMs in X-ray clusters are isothermal. Indeed, isothermality is generally assumed when fitting β -models to X-ray surface brightness profiles. This would be a surprising result, if true, since in gravitationally-bound systems the temperature usually rises toward the center. It would imply that some mechanism such as thermal conduction was efficient in transporting energy outward and depositing it at large radii. Radiation cannot do the job as the plasma is optically thin to X-rays. Analyses have shown that thermal conduction is incapable of rendering a cluster isothermal even if the full classical electron conductivity is assumed (e.g., Loeb 2002).

The non-radiative simulations of Navarro, Frenk & White (1995) found that the temperature profile is nearly isothermal in the region that emits most

of the X-rays $r < 0.4r_{vir}$, but then drops to about one-half the central value at the virial radius. Results of other SPH codes in the Santa Barbara cluster comparison project generally agreed, however with substantial differences in the central value. Some SPH codes found a central dip in temperature while others did not. High resolution grid-based codes, such as AMR, agree well with the SPH results beyond $r = 0.4r_{vir}$, but continue to rise to small radius (Fig. 2). Thus, the issue of core temperature profiles is not yet settled, even for non-radiative simulations.

Observationally, the issue is also clouded. Markevitch et al. (1998) found evidence of decreasing temperature profiles in a sample of nearby hot clusters (> 3.5 keV) observed with ASCA. A subsample of 17 regular/symmetric clusters displayed remarkably similar temperature profiles (when normalized and scaled by the virial radius) consistent with $T \propto [1 + (r/r_c)^2]^{-3\beta(\gamma-1)/2}$ where $\gamma = 1.24^{+0.20}_{-0.12}$ and $\beta = 2/3$. The typical decrease is therefore a factor of ~ 2 in going from 1 to 6 core radii (or .09 to 0.5 virial radii). This result remains controversial as three subsequent studies of large samples of clusters concluded that the majority of cluster temperature profiles show little, or no, decrease with radius (Irwin, Bregman, & Evrard 1999; White 2000; Irwin & Bregman 2000). Most recently, De Grandi & Molendi (2002) have presented a composite temperature profile based on *BeppoSAX* data which exhibits an isothermal core and then decreases quickly.

Loken et al. (2002) computed a statistical sample of non-radiative X-ray clusters in two cosmologies (LCDM and SCDM) using AMR. The temperature profiles are well fit by $T/T_o = 1.3[1+1.5r/r_{vir}]^{-1.6}$. This fit is in excellent agreement with Markevitch et al. (1998) and also in good agreement with the *BeppoSAX* data outside $r = 0.2r_{vir}$. The simulation results and comparison with data are shown in Fig. 3. These results suggest that relaxed X-ray clusters should have a universal temperature profile outside the core, inside which additional heating and cooling processes may operate.

4 Simulations Including Preheating and Radiative Cooling

4.1 Preheating

Given the failure of non-radiative simulations to reproduce the observed L_x-T relation, one is driven to consider the effect of other physics. One possibility is an early epoch of preheating (David, Jones & Forman 1991; Evrard & Henry 1991; Kaiser 1991; White 1991) that raises the entropy of the intergalactic medium prior to it being incorporated into a cluster. The idea is that preheating introduces an entropy floor that breaks the self-similarity between dark matter and ICM on different mass scales. If this entropy floor were larger than the core entropy produced by gravitational heating in low mass clusters but not so in high mass clusters, the central densities and hence luminosities of low mass clusters would be reduced relative to high mass clusters,

thus steepening the $L_x - T$ relation. This has been confirmed numerically by Navarro et al. (1995) and Pierre et al. (1999). An extensive recent study by Bialek, Evrard & Mohr (2001) systematically varied the initial entropy S_i in a grid of simulations and found that the $L_x - T$ relation, as well as the X-ray size-temperature and mass-temperature relations steepen monotonically with S_i . They found that the three observed relations could be satisfied with $S_i \in 55 - 150 \text{ keV cm}^{-2}$. These levels compare favorably to observational determinations of core ICM entropy by Lloyd-Davies et al. (2000).

4.2 Radiative Cooling, Cooling Flows, and Cooling Catastrophes

The potential impact of radiative cooling by the ICM has been recognized for many years (Cowie & Binney 1977, Fabian & Nulsen 1977). The X-ray emitting gas is trapped in approximate hydrostatic equilibrium in the cluster's potential well. A "cooling flow" is believed to form as the radiating gas loses pressure support and flows inward to higher density values thus accelerating the cooling rate. In cooling flow clusters, typically, the gas within approximately 100 kpc of the center has a cooling time which is less than the age of the cluster. This theoretical scenario has been extensively developed (see Fabian 1994 for a review) and observations of X-ray clusters with central brightness excesses are routinely analyzed with the framework of these models (e.g., David et al. 2001).

In principle, cosmological hydrodynamic simulations including radiative cooling should see these cooling flows develop self-consistently. This effort has not been entirely successful and the implications of this have not yet been sorted out. Thomas & Couchman (1992) and Katz & White (1993) did the first SPH simulations with cooling and found that an unresolved lump of cold (10^4 K) gas forms in the cluster center. In the simulation of Katz & White the lump contained 30% of the baryons causing the integrated luminosity to be too high for a cluster of that temperature. Similar results have been obtained by Sugimotohara & Ostriker (1998) and Valdarnini (2002) using higher resolution SPH simulations. While superficially resembling a cooling flow cluster, it is clear that in the absence of star formation and feedback, too much gas cools. Solutions to the so-called overcooling problem have been proposed, including conversion of gas to stars (Valdarnini 2002), feedback from star formation, and heating from a central AGN.

Pearce et al. (2000) discussed a purely numerical origin of the overcooling problem due to the way SPH treats phase boundaries (see also Springel & Hernquist 2002). If one imagines how an ideal discontinuity between a cool, dense phase and a hot diffuse phase is represented in SPH, one realized that the kernel averaging will smear the discontinuity over several smoothing lengths and thereby create a region of intermediate density and temperature of that thickness. Since the X-ray emissivity is proportional to $\rho^2 T^{1/2}$, the numerically-induced layer's emissivity will be boosted and will radiate energy at a rate which is proportional to the thickness of the layer. In reality, the

layer would be a few collision mean free paths thick but numerically is it much larger. The enhanced cooling thereby leads to too much hot gas being converted to cool gas.

In order to overcome this problem, Pearce et al. (2000) carried out simulations of cooling clusters with a formulation that manually limits how much gas may cool. Using values from observed clusters, they found that cooling had a *global effect* on the cluster profiles. Namely, that cooling produces an inflow of high entropy gas from the outer parts of the cluster, raising the cluster temperature and decreasing the X-ray luminosity. Outside the cooling radius, the temperature profiles were found to be in good agreement with Markevitch et al. (1998); while inside the cooling radius, the temperature decreased toward the center as seen in cooling flow clusters.

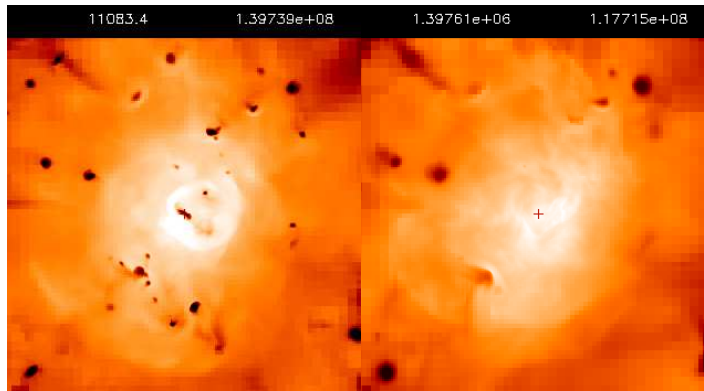


Fig. 4. Emission-weighted temperature image for a cluster simulated (a) with, and (b) without radiative cooling included. The image is 5 Mpc on a side.

Does the presence of cool gas in clusters cores necessarily imply the existence of cooling flows? Motl et al. (2002) studied this question with high-resolution hydrodynamic AMR simulations and concluded no. Motl et al. computed two massive X-ray clusters in a Λ CDM universe with and without radiative cooling included. The simulations achieved a spatial resolution of 22 kpc in a cosmological volume 365 Mpc on a side. Fig. 4 shows a comparison of the non-radiative and radiative simulations. The cooling simulation produces lumps of cooler gas that are associated with subclusters. These subclusters merge hierarchically and survive their passage through the ICM. Those on radial orbits find their way to the cluster core where they deposit their cool gas. Hierarchical formation naturally explains the high frequency of cooling cores in rich galaxy clusters despite the fact that a majority of these cluster show evidence of substructure which is believed to arise from recent merger activity. The simulations also produce cooling fronts, “bullets”, and filaments (Markevitch, these proceedings.)

5 Simulations Including Galaxy Formation and Feedback

Although galaxies comprise a small fraction (15–25%) of the baryons in a rich cluster of galaxies (David et al. 1990), they may have a disproportionate effect on the ICM. Observations indicate ICM metallicities of $Z \sim 0.3Z_{\odot}$ (e.g., Edge & Stewart 1991). These metals imply supernova enrichment of the gas either before, during, or after cluster assembly. Mushotzky & Lowenstein (1997) report little evolution in cluster metallicities out to $z \sim 0.3$, suggesting that the gas was enriched prior to cluster assembly. Supernova enrichment would naturally be accompanied by supernova heating. A key question therefore is whether this heating is sufficient to provide the entropy floor observed in clusters (Lloyd-Davies et al. 2000) as has been suggested by Ponman et al. (1999).

5.1 Effects on Structure

Numerical simulations of cluster formation including galaxy formation and feedback are in their infancy. Nonetheless, they show signs of producing clusters that are more in line with observations and eliminating the overcooling problem encountered in cooling-only simulations (Valdarnini 2002). The first study of this sort was by Metzler & Evrard (1994). Because galaxies form on scales that are unresolved in standard cluster simulations, special care must be made in how galaxies are represented. Metzler & Evrard (1994) put the galaxies in “by hand” at locations corresponding to peaks in the initial density field that would eventually form L_* galaxies. A galaxy particle was introduced at each of these locations in the initial data and evolved dynamically along with the gas and dark matter particles. A total of 108 galaxy particles fed back energy and metals according to a user-supplied history. These authors compared evolutions for a cluster with “extreme feedback” and without. Extreme feedback consisted of assuming a constant feedback level for $0 \leq z \leq 4$ and a wind luminosity of 4×10^{42} erg/s for a $10^{10}L_{\odot}$ galaxy. They found that feedback raised the entropy of the ICM, establishing an entropy floor in the core. This reduced the gas density in the core and hence the integrated luminosity. The emission weighted temperature increased only 15%, and the X-ray morphology of the cluster was relatively unchanged.

Lewis et al. (2000) carried out TREESPH simulations of the formation of a Virgo-mass cluster in a standard CDM cosmology including star formation and energy feedback. The simulations convert localized regions of gas which are cooling and collapsing rapidly into collisionless star particles according to the recipe described in Katz, Weinberg & Hernquist (1996). In this approach, an SPH particle is eligible to form stars if it exceeds a threshold density and overdensity, and if the particle’s neighborhood is collapsing and Jeans unstable. If these conditions are met, gas is turned into stars at a rate $d \ln$

$\rho_g/dt = -c_*/t_g$, where t_g is the maximum of the local dynamical time and cooling time. The advantage of this approach is that in principle the star formation histories of individual galaxies can be computed, as opposed to the constant rate assumption of Metzler & Evrard (1994). The disadvantage is that quite high mass and spatial resolution are required, and it is unclear whether simulations have achieved the necessary resolution for convergence.

Lewis et al. report on simulations with and without galaxy feedback with a spatial resolution of $14h^{-1}$ kpc. They find that inclusion of cooling and star formation affects the structure of the entire cluster, in agreement with Pearce et al. (2000). 30% of the baryons are converted to stars forming a massive galaxy at the center of the cluster, altering the cluster potential well. With the low entropy gas thus converted into a pressureless component, the higher entropy gas settles into the core region. Compared to the non-radiative model, they find this structural readjustment leads to a 20% higher emission-weighted temperature and a 30% higher X-ray luminosity. This result is partially in conflict with the results of Pearce et al. (2000), who found an increase in $\langle T_x \rangle$ and a *decrease* in L_x . Interestingly, the concentration of baryons in the core was found to actually steepen the dark matter profile relative to an NFW profile inside ~ 30 kpc.

Lewis et al. found that star formation and feedback *steepens* the ICM temperature profile in the inner regions, a result confirmed by Valdarnini (2002). However, the latter author found that cooling creates a central temperature inversion within $\sim 50 - 100$ kpc, which he interpreted as a cooling flow. Recent *BeppoSAX* observations of cooling flow cluster temperature profiles (De Grandi & Molendi 2002; cf. Fig. 3b) show this central dip in what is otherwise an isothermal core extending to $\sim 0.2r_{vir} \sim 400$ kpc, in rough agreement with the simulations.

5.2 Metal Enrichment

If a cluster formed out uniformly mixed intergalactic material, and if no subsequent injection of metals took place after the cluster virialized, then one would expect uniform ICM metallicity profiles. If, on the other hand, the infalling gas was enriched locally by the galaxies which ultimately end up in the cluster, then one would expect a strong negative radial gradient. If enrichment occurred after cluster assembly, then the high density of galaxies in the inner parts of the cluster would accentuate any pre-existing metallicity gradient. The same could be said for cooling flows. Thus, metallicity gradients in clusters can in principle probe the star formation and chemical enrichment history of a large sample of the universe (Mushotzky & Lowenstein 1997).

Metal enrichment was included in the simulations of Metzler & Evrard (1994). In their “extreme feedback” model, they assumed a constant, galaxy mass normalized, metal injection rate from $z=4$ to 0. The transport of metals from the galaxy particle occurs by virtue of the SPH smoothing operation rather than resolved hydrodynamically. To the extent that the smoothing

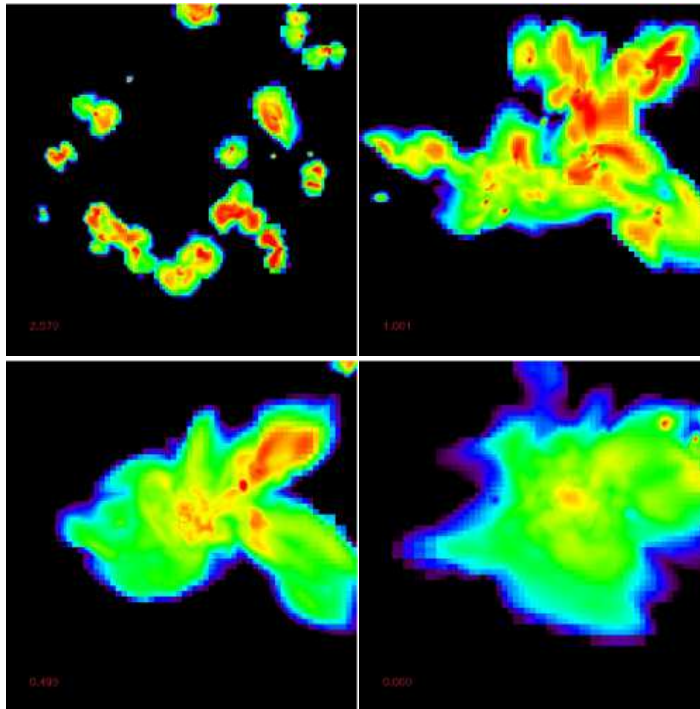


Fig. 5. Evolution of metallicity field in an AMR simulation of the Santa Barbara cluster including cooling, star formation, and feedback. *upper left to lower right:* $z = 2.6, 1, 0.5, 0$.

length exceeds/underestimates the physical mixing scale, the resulting metallicity distribution will be smoother/less smooth than nature would produce. A simulation with a minimum smoothing length of 110 kpc produced a metallicity distribution which is strongly peaked about the cluster center. In units of the wind metallicity—a free parameter—the metallicity varied from 0.5 in the center to 0.1 at 1 Mpc. Steeper gradients could be achieved by reducing the amount of mixing.

The simulations of Valdarnini (2002) included chemical enrichment from galaxies formed “self-consistently” in the protocluster. The $z=0$ cluster exhibited a metallicity distribution that varied from solar at the center to < 0.1 solar at $r = 100$ kpc. This is much steeper than what is observed (De Grandi & Molendi 2001). A likely explanation for this disagreement is that the galaxy population is severely undersampled such that the chemical enrichment is dominated by the massive central galaxy.

Fig. 4 shows the results of an AMR simulation including cooling, star formation, feedback and chemical enrichment which produces a metallicity distribution more in line with observations (O’Shea et al. 2002). The Santa

Barabara cluster was rerun with the star formation recipe of Cen & Ostriker (1993). The minimum spatial resolution is 15.6 kpc, which is sufficient to resolve the formation of a dozen massive galaxies that enrich the IGM prior to cluster collapse. Metallicity is tracked as a separate fluid dynamic field, and therefore mixing occurs hydrodynamically. Fig. 4 shows the evolution of the metallicity field. At high redshifts, a population of ~ 20 galaxies enriches the IGM over a region ~ 8 Mpc in diameter. The metallicity distribution is extremely inhomogeneous at this time. As time goes on, this gas is drawn into the cluster and mixed with pristine gas. The final metallicity distribution exhibits a mild gradient, dropping from $0.3Z_{\odot}$ at the center to $0.1Z_{\odot}$ at $r = 0.3r_{vir}$. This gradient is in good agreement with the cooling flow cluster sample of De Grandi & Molendi (2001) although the normalization is too low by a factor of 2.

Acknowledgements: I wish to thank my students and collaborators for their contributions to the work described here: Greg Bryan, Jack Burns, Chris Loken, Patrick Motl, Erik Nelson and Brian O'Shea.

References

1. Anninos P, Norman ML. 1996. ApJ 459:12-26
2. Bertschinger, E. 1998. Ann. Rev. Astron. Astrophys. 36:599-654.
3. Bryan, G. L. 1999. IEEE Computing in Science and Engineering, Vol. 1, No. 2, p. 33.
4. Bryan GL, Cen R, Norman ML, Ostriker JP, Stone JM 1994. ApJ 428:405
5. Bryan GL, Klypin A, Loken C, Norman ML, Burns O. 1994. ApJ Lett. 437:L5-8
6. Bryan G, Norman M, Stone J, Cen R, Ostriker J. 1995. Comp. Phys. Commun. 89:149-68
7. Bryan, G. & Norman, M. 1997. Computational Astrophysics; ASP Conference Series #123, edited by D. A. Clarke and M. J. West., p. 363
8. Bryan, G. & Norman, M. 1999. in *Structured Adaptive Mesh Refinement Grid Methods*, eds. N. Chrisochoides et al., IMA Conference Series
9. Cavaliere A, Fusco-Femiano R 1976. A&A 49:137
10. Cen, R. & Ostriker, JP 1993. ApJ 417:404-414
11. Cowie LL, Binney, J 1977. ApJ 215:723
12. David LP, Arnaud K, Forman W, Jones C 1990. ApJ 356:32
13. David LP, Forman W, Jones C, 1991. ApJ 380:39
14. David LP, Slyz A, Jones C, Forman W, Vrtelek SD, Arnaud AC 1993. ApJ 412: 479
15. David, LP; Nulsen, PE; McNamara, BR; Forman, W; Jones, C; Ponman, T; Robertson, B; Wise, M 2001. ApJ 557:546
16. De Grandi S, Molendi S 2001. ApJ 551:153
17. De Grandi S, Molendi S 2002. ApJ 567:163
18. Edge AC, Stewart GC 1991. MNRAS 252:428
19. Eke VR, Navarro JF, Frenk CS 1998. ApJ 503:569
20. Evrard AE. 1988. MNRAS 235:911-34

21. Evrard AE. 1990. ApJ 363:349-66
22. Evrard AE, Henry JP 1991. ApJ 383:95
23. Evrard,AE, Metzler C, Navarro JP 1996. ApJ 469:494
24. Fabian AC 1994. ARAA 32:277
25. Fabian AC, Nulsen PE 1977. MNRAS 180:479
26. Forman W, Jones C 1982. ARAA 20:547
27. Frenk, CS, White, SDM, et al. 1999. ApJ, 525, 544
28. Gnedin NY. 1995. ApJ Suppl. 97:231-57
29. Irwin JA, Bregman J 2000. ApJ 538:543
30. Irwin JA, Bregman J, Evrard AE 1999. ApJ 519:518
31. Kaiser N 1986. MNRAS 222:323
32. Kaiser N 1991. ApJ 383:104
33. Kang, H; Cen, R; Ostriker, JP; Ryu, D 1994. ApJ 428:1-16
34. Katz N, White SDM 1993. ApJ 412:455
35. Lewis GF, Babul A, Katz N, Quinn T, Hernquist L, Weinberg D 2000. ApJ 536:623
36. Lloyd-Davies EJ, Ponman TJ, Cannon DB 2000. MNRAS 315:689
37. Loeb A 2002. NewA 7:279
38. Loken C, Norman ML, Nelson, E, Burns JO, Bryan GL, Motl P 2002. ApJ in press (astro-ph/0207095)
39. Markevitch M, Forman W, Sarazin CL, Vikhlinin A 1998. ApJ 503:77
40. Metzler CA, Evrard AE 1994. ApJ 437:564
41. Motl P. et al. 2002, preprint
42. Navarro JF, Frenk CS, White SDM. 1995. MNRAS 275:720-40
43. Navarro JF, Frenk CS, White SDM. 1997. MNRAS 275:720-40
44. Norman ML, Bryan GL 1998. in *The Radio Galaxy M87*, eds. H-J Röser & K. Meisenheimer, LNP 530, (Springer: Heidelberg), p. 106
45. O'Shea B, Nelson E, Norman ML 2002, in preparation
46. Pearce FR, Thomas PA, Couchman HMP, Edge AC 2000. MNRAS 317:1029
47. Pen, U-L 1995. ApJS 100:269
48. Pierre M; Bryan GL; Gastaud R 1999. A&A 356:403
49. Ponman TJ; Cannon DB; Navarro, JF 1999. Nature 397:135
50. Ryu D, Ostriker JP, Kang H, Cen R. 1993. ApJ 414:1-19
51. Pen U-L. 1995. ApJ Suppl. 100:269-80
52. Sarazin CL 1986. Rev. Mod. Phys. 58:1
53. Springel V, Hernquist L 2002. MNRAS 333:649
54. Sugihara T, Ostriker JP 1998. ApJ 507:16
55. Tegmark M, Zaldarriaga M 2002. preprint (astro-ph/0207047)
56. Thomas PA Couchman, HMP 1992. MNRAS 257:11
57. Valdarnini R 2002. ApJ 567:741
58. White RE 1991. ApJ 367:69
59. White DA 2000. MNRAS 312:663